INT. J. NUM. METH. HEAT FLUID FLOW, VOL. 5, 685–704 (1995)

CHEBYSHEV SERIES SOLUTION FOR RADIATIVE TRANSPORT IN A MEDIUM WITH A LINEARLY ANISOTROPIC SCATTERING PHASE FUNCTION

T. LACLAIR† AND J. I. FRANKEL‡

† *Project Engineer Phillip Laboratory USAF, 3550 Aberdeen Ave. SE, Building 30117, Kirtland AFB, NM 87117-5776, USA*

‡ *Department of Mechanical and Aerospace Engineering, University of Tennessee, Knoxville, Knoxville, TN 37996-2210, USA*

ABSTRACT

One-dimensional radiative heat transfer is considered in a plane-parallel geometry for an absorbing, emitting, and linearly anisotropic scattering medium subjected to azimuthally symmetric incident radiation at the boundaries. The integral form of the transport equation is used throughout the analysis. This formulation leads to a system of weakly-singular Fredholm integral equations of the second kind. The resulting unknown functions are then formally expanded in Chebyshev series. These series representations are truncated at a specified number of terms, leaving residual functions as a result of the approximation. The collocation and the Ritz-Galerkin methods are formulated, and are expressed in terms of general orthogonality conditions applied to the residual functions. The major contribution of the present work lies in developing quantitative error estimates. Error bounds are obtained for the approximating functions by developing equations relating the residuals to the errors and applying functional norms to the resulting set of equations. The collocation and Ritz-Galerkin methods are each applied in turn to determine the expansion coefficients of the approximating functions. The effectiveness of each method is interpreted by analyzing the errors which result from the approximations.

KEY WORDS Heat transfer Scattering medium Collocation method Chebyshev series solution

INTRODUCTION

The transfer of heat which is due to thermal radiation is referred to as radiation heat transfer and is a significant mode of heat transfer in many modern engineering applications. Some specific areas in which radiation heat transfer is important include the design and analysis of energy conversion systems such as furnaces, combustors, solar energy conversion devices, and engines, where high temperatures must exist in order to improve thermodynamic efficiency of the processes, and where the other modes of heat transfer may also be significant. Also, for the processing of materials such as glass, crystals, and metals, in which elevated temperatures are used to remove impurities from the material and temperatures must be controlled to enhance crystal formation for improved properties of the material, radiation is an important consideration. The use of materials such as optical components and fibrous and porous insulations, where the distribution of heat determines the operational performance of the material, requires knowledge of the radiative effects which may influence the temperature within these materials. In both nuclear reactor safety, where the temperatures must constantly be monitored and controlled, and

0961–5539/95/080685–20$2.00

Received January 1994
Revised July 1994

diagnostics such as spectroscopy, remote sensing of atmospheric pollutants, and satellite reconnaissance, where radiation fields are measured and analyzed, radiation heat transfer is a very important factor[1]. Numerous other applications may also be found in the literature.

Radiation heat transfer developed primarily due to activities involving astronomy and astrophysics. Early analytical work was performed by Lord Rayleigh in 1871, Schuster in 1905, and Schwartzschild in 1906[2]. Since that time the importance of thermal radiation has increased in engineering owing to increased high temperature applications. Many analyses of thermal radiation in an absorbing, emitting, and scattering medium have appeared in the literature[3–8]. Complete treatment of this problem, however, was next to impossible prior to the development of modern digital computers, and often several simplifying assumptions were made in order to solve the equations. Essentially identical equations also arise in neutron transport, thus additional investigations for solution of the equations have been made in this field as well[2].

Numerous analytical and numerical approaches have been offered for solving the linearized Boltzmann transport equation. Case's normal mode expansion[9–12] can supply reliable analytical solutions for idealized problems. The facile method, i.e., F_N method[13], has been applied successfully to produce highly accurate results but has only been implemented on relatively simple geometries. Again, this approach is very useful for obtaining benchmark results but does not appear to be tractable to difficult geometries. The conventional P_N method[10,11,14] is an expansion based method which has been used for solving numerous pertinent problems in radiative and neutron transport. Again, irregular geometries may cause some difficulties unless some modifications are made.

Galerkin methods[5,6,15–17] have been developed in the context of an integral formulation where Fredholm integral equations of the second kind are produced in terms of the Legendre moments of the intensity. Power series expansions in the optical variable have been used often in this context[6,15,16]. Legendre polynomials of the first kind were used as basis functions by Cengel and Ozisik[17] in developing a Galerkin solution of radiative transport in a slab geometry. Recently, Frankel[5] illustrated that Chebyshev polynomials of the first kind can be used as the basis functions. Theoretical considerations concerning error bounds and convergence rates were reported in that study when considering an isotropically scattering phase function. The use of Fourier transforms[18] and eigenfunctions expansions[19] have been implemented to produce accurate results in a slab geometry. Thynell and Ozisik[19] considered several highly anisotropic scattering phase functions and developed accurate solutions based on eigenfunction expansions. It has been observed[14] that an expansion in the optical variable produces fast convergence. However, little theoretical work has appeared quantifying the rate of convergence and the accurate establishment of error bounds especially with regard to anisotropic scattering.

In practical applications, the most direct solution procedure is based on the discrete-ordinates method[10,11]. This method is well-suited to many physical situations. The transport equation is discretized by using a numerical quadrature for approximating the integrals while a finite difference method is typically used for approximating the spatial variable.

Many of the currently proposed solution methods attempt to determine the radiative intensity distribution throughout the medium of interest and subsequently determine the radiative flux and divergence of the radiative flux to determine heat transfer rates and temperature distributions. However, by first manipulating the radiative transfer equation into an equivalent integral form, we can reduce the number of independent variables and obtain the quantities of interest much more readily than from the radiative intensity. Therefore, this method allows us to both simplify the analysis of the radiation problem itself and gives us the principal quantities of engineering interest without extensive further calculation.

The purpose of the present exposition is threefold: (i) to develop a simple yet elegant expansion method using Chebyshev polynomials of the first kind as a set of orthogonal basis functions, (ii) to present a new and informative residual/error analysis which is useful in assessing performance/accuracy, and (iii) to implement and demonstrate the utility of symbolic computation in arriving at the numerical results.

INTEGRAL FORMULATION

In this section, we present the integral form of the radiative transfer equation. This integral formulation reduces the number of independent variables in the unknown functions and leads to much simpler calculation of many quantities of engineering interest, such as the radiative flux and the divergence of the radiative flux. Furthermore, there appears to be greater stability in the calculations of these quantities as obtained from the integral formulation than from the differential form.

In a plane-parallel, linear-anisotropically scattering, absorbing, and emitting medium of optical thickness τ_D subject to transparent boundary conditions, the appropriate[4,8] integral form becomes:

$$G_0(\tau) = F_0(\tau) + \frac{\omega}{2}\left[a_0 \int_{\tau_0=0}^{\tau_D} E_1(|\tau-\tau_0|)G_0(\tau_0)d\tau_0 + a_1 \int_{\tau_0=0}^{\tau} E_2(\tau-\tau_0)G_1(\tau_0)d\tau_0 - a_1 \int_{\tau_0=\tau}^{\tau_D} E_2(\tau_0-\tau)G_1(\tau_0)d\tau_0\right], \qquad \tau \in [0, \tau_D] \tag{1a}$$

and

$$G_1(\tau) = F_1(\tau) + \frac{\omega}{2}\left[a_0 \int_{\tau_0=0}^{\tau} E_2(\tau-\tau_0)G_0(\tau_0)d\tau_0 - a_0 \int_{\tau_0=\tau}^{\tau_D} E_2(\tau_0-\tau)G_0(\tau_0)d\tau_0 + a_1 \int_{\tau_0=0}^{\tau_D} E_3(|\tau-\tau_0|)G_1(\tau_0)d\tau_0\right], \qquad \tau \in [0, \tau_D] \tag{1b}$$

where

$$F_n(\tau) = \int_{\mu=0}^{1} P_n(\mu)[f_1(\mu)e^{-\tau/\mu} + (-1)^n f_2(\mu)e^{-(\tau_D-\tau)/\mu}]d\mu + \int_{\tau_0=0}^{\tau_D} s(\tau_0)K_{0,n}(\tau-\tau_0)d\tau_0, \qquad n = 0, 1, \ldots \tag{1c}$$

and

$$K_{m,n}(\tau-\tau_0) = R_{m,n}(\tau-\tau_0)Q_{m,n}(|\tau-\tau_0|) \tag{1d}$$

with

$$R_{m,n}(\tau-\tau_0) = \begin{cases} 1, & \tau > \tau_0 \\ (-1)^{m+n}, & \tau < \tau_0 \end{cases} \tag{1e}$$

where the partial kernel functions $Q_{m,n}(|\tau-\tau_0|)$ reduce to:

$$\begin{aligned} Q_{0,0}(|\tau-\tau_0|) &= E_1(|\tau-\tau_0|) \\ Q_{0,1}(|\tau-\tau_0|) &= Q_{1,0}(|\tau-\tau_0|) = E_2(|\tau-\tau_0|) \\ Q_{1,1}(|\tau-\tau_0|) &= E_3(|\tau-\tau_0|) \end{aligned} \tag{1f}$$

Here, the unknown functions, $G_m(\tau)$, $m = 0, 1$ are the mth Legendre moments of the intensity and are defined[8] as:

$$G_m(\tau) \equiv \int_{\mu'=-1}^{1} P_m(\mu')I(\tau, \mu')d\mu' \tag{2}$$

where $P_m(\mu)$ is the mth Legendre polynomial of the first kind and $I(\tau, \mu)$ is the local radiative intensity. The boundary conditions $f_1(\mu)$ and $f_2(\mu)$ correspond to externally incident, azimuthally-symmetric radiation[9], namely:

$$I(0, \mu) = f_1(\mu), \qquad \mu > 0 \tag{3a}$$

$$I(\tau_D, -\mu) = f_2(\mu), \qquad \mu > 0 \tag{3b}$$

whereas the function $s(\tau)$ is given by:

$$s(\tau) = (1-\omega)\frac{n^2\sigma T^4(\tau)}{\pi}, \qquad \tau \in [0, \tau_D] \tag{4}$$

where ω is the single-scattering albedo, n is the index of refraction, σ is the Stefan-Boltzmann constant, and T is the local temperature in the medium at optical depth τ. The exponential integral functions appearing in (1) are defined as[10]:

$$E_n(z) = \int_{\mu=0}^{1} e^{-z/\mu}\mu^{n-2}d\mu, \qquad z \geqslant 0, n = 1, 2, \ldots \tag{5}$$

The constants a_0, a_1 are associated with the linearly anisotropic scattering phase function, namely[9]:

$$P(\mu, \mu') = \sum_{m=0}^{1} a_m P_m(\mu)P_m(\mu') = a_0 + a_1\mu\mu' \tag{6}$$

where $P(\mu, \mu')$ is the scattering phase function under our imposed constraints.

The phase function is normalized by requiring that $a_0 = 1$. When $a_1 = -1$ the scattering is said to be "highly backward", while when $a_1 = 1$ the scattering is said to be "highly forward". The case when $a_1 = 0$ represents isotropic scattering. When $|a_1| \geqslant 1$ in linearly anisotropic scattering, the phase function is actually an approximation of a higher-order phase function which describes highly-forward or highly-backward scattering. This approximation yields accurate results in many important applications[3]. The attributes of the integral formulation are well documented[4,5,6,8]. Equations (1a), (1b) represent a set of linear Fredholm integral equations of the second kind. The kernel $E_1(|\tau-\tau_0|)$ shown in (1a) contains a logarithmic singularity as $\tau_0 \to \tau$.

At this point, it is convenient to transform the physical domain from $\tau \in [0, \tau_D]$ to $x \in [-1, 1]$ in order to introduce our expansion of the unknown functions in terms of a Chebyshev series. Transforming the domain via a linear transformation, we let:

$$x \equiv \frac{2\tau - \tau_D}{\tau_D} \tag{7a}$$

$$x_0 \equiv \frac{2\tau_0 - \tau_D}{\tau_D} \tag{7b}$$

and define:

$$\alpha \equiv \frac{\tau_D}{2}$$

noting that $x = \frac{\tau}{\alpha} - 1$. We therefore define:

$$G_n^*(x) \equiv G_n\left(\alpha x + \frac{\tau_D}{2}\right) = G_n(\alpha(x+1)) \tag{8a}$$

and

$$F_n^*(x) \equiv F_n(\alpha(x+1)), \qquad n = 0, 1 \tag{8b}$$

The transformed equations governing the zeroth and first Legendre moment of the intensity become:

$$G_0^*(x) = F_0^*(x) + \frac{\alpha\omega}{2}\left[a_0 \int_{x_0=-1}^{1} E_1(\alpha|x-x_0|)G_0^*(x_0)dx_0 + a_1 \int_{x_0=-1}^{x} E_2(\alpha(x-x_0))G_1^*(x_0)dx_0 - a_1 \int_{x_0=x}^{1} E_2(\alpha(x_0-x))G_1^*(x_0)dx_0\right], \qquad x\in[-1,1] \tag{9a}$$

$$G_1^*(x) = F_1^*(x) + \frac{\alpha\omega}{2}\left[a_0 \int_{x_0=-1}^{x} E_2(\alpha(x-x_0))G_0^*(x_0)dx_0 - a_0 \int_{x_0=x}^{1} E_2(\alpha(x_0-x))G_0^*(x_0)dx_0 + a_1 \int_{x_0=-1}^{1} E_3(\alpha|x-x_0|)G_1^*(x_0)dx_0\right], \qquad x\in[-1,1] \tag{9b}$$

We are now in a position to formally expand $G_0^*(x)$ and $G_1^*(x)$ in terms of Chebyshev series representations. Thus, we write:

$$G_0^*(x) = \sum_{i=0}^{\infty} b_i T_i(x), \qquad x\in[-1,1] \tag{10a}$$

and

$$G_1^*(x) = \sum_{i=0}^{\infty} c_i T_i(x), \qquad x\in[-1,1] \tag{10b}$$

where $T_n(x)$ is the nth Chebyshev polynomial of the first kind, given by [20–22]:

$$T_n(x) \equiv \cos(n\cos^{-1}x), \qquad n=0,1,2,\ldots \tag{11}$$

To simplify the notation we express (9a) and (9b) in operator form:

$$G_0^* = F_0^* + a_0\kappa_0 G_0^* + a_1\kappa_1 G_1^* \tag{12a}$$

and

$$G_1^* = F_1^* + a_0\kappa_1 G_0^* + a_1\kappa_2 G_1^* \tag{12b}$$

where we interpret our symbolic notation as:

$$\kappa_j\psi \equiv \int_{y=-1}^{1} k_j(x,y)\psi(y)dy, \qquad x\in[-1,1] \tag{13}$$

where $k_j(x, y)$ are the appropriate kernels and $\psi(y)$ is any arbitrary function.

We seek an approximate solution to $G_m^*(x)$, $m=0, 1$, by truncating the infinite series representations for $G_m^*(x)$, $m=0, 1$, at a certain order, say N, leaving:

$$G_0^N(x) = \sum_{i=0}^{N} b_i^N T_i(x), \qquad x\in[-1,1] \tag{14a}$$

and

$$G_1^N(x) = \sum_{i=0}^{N} c_i^N T_i(x), \qquad x\in[-1,1] \tag{14b}$$

where b_i^N and c_i^N are approximations to b_i and c_i, respectively. Thus, we may express (12a) and (12b) as:

$$G_0^N = F_0^* + a_0\kappa_0 G_0^N + a_1\kappa_1 G_1^N - R_0^N \tag{15a}$$

and

$$G_1^N = F_1^* + a_0\kappa_1 G_0^N + a_1\kappa_2 G_1^N - R_1^N \tag{15b}$$

respectively, where we have introduced the residual functions R_0^N and R_1^N to account for the error resulting from the approximation.

Substituting (14a) and (14b) into (15a) and (15b) and, formally interchanging orders at summation and integration produces:

$$R_0^N(x) + \sum_{i=0}^{N} b_i^N T_i(x) = F_0^*(x) + \frac{\alpha\omega}{2}\left[a_0 \sum_{i=0}^{N} b_i^N \int_{x_0=-1}^{1} E_1(\alpha|x-x_0|)T_i(x_0)dx_0 + a_1 \sum_{i=0}^{N} c_i^N \left\{\int_{x_0=-1}^{x} E_2(\alpha(x-x_0))T_i(x_0)dx_0 - \int_{x_0=x}^{1} E_2(\alpha(x_0-x))T_i(x_0)dx_0\right\}\right], \quad x\in[-1,1] \tag{16a}$$

and

$$R_1^N(x) + \sum_{i=0}^{N} c_i^N T_i(x) = F_1^*(x) + \frac{\alpha\omega}{2}\left[a_0 \sum_{i=0}^{N} b_i^N \left\{\int_{x_0=-1}^{x} E_2(\alpha(x-x_0))T_i(x_0)dx_0 - \int_{x_0=x}^{1} E_2(\alpha(x_0-x))T_i(x_0)dx_0\right\} + a_1 \sum_{i=0}^{N} c_i^N \int_{x_0=-1}^{1} E_3(\alpha|x-x_0|)T_i(x_0)dx_0\right], \quad x\in[-1,1] \tag{16b}$$

We now notice that, for specified boundary conditions such that $F_0^*(x)$ and $F_1^*(x)$ are known functions given by (1c), we have reduced the problem to a point where all integrals involved can be determined analytically. These expressions are developed in the next section of analysis. Therefore, we are in an excellent position to perform a numerical analysis to determine the unknown expansion coefficients b_i^N and c_i^N, $i=0, 1, \ldots, N$, by placing some type of restriction on the functions $R_0^N(x)$ and $R_1^N(x)$.

COLLOCATION AND RITZ-GALERKIN METHODS

In this section, we present a systematic approach for determining the unknown expansion coefficients shown in (16a) and (16b). Projection methods encompass techniques such as collocation, Galerkin methods, and least-squares procedures and have been the topic of much research[23–27]. The proposed numerical methods used here are presented in a weighted-residual framework. An exact solution is given if the residual functions are identically zero for $x\in[-1, 1]$. This is not possible for our finite Chebyshev series approximation unless the actual solution is a linear combination of the Chebyshev polynomials $\{T_n(x)\}$, $n=0, 1, \ldots, N$. Therefore, we attempt to minimize the residuals $R_0^N(x)$ and $R_1^N(x)$ in some manner. A particular expansion method is defined by any restriction imposed on the residual functions shown in (16a), (16b). We wish to determine the unknown expansion coefficients $\{b_n^N\}$ and $\{c_n^N\}$, $n=0, 1, \ldots, N$, in such a manner that some measure of the residual functions is small. A systematic way of expressing this is to require that the orthogonality condition[5]:

$$\langle R_j^N(x), \varphi_k(x)\rangle_{w_k} = 0, \qquad j = 0, 1 \textit{ and } k = 0, 1, \ldots, N \tag{17}$$

be enforced for $i = 0, 1, \ldots, N$. For the point-collocation method $w_k(x) = \delta(x - x_k)$ and $\varphi_k(x) = 1$, where $\delta(x)$ is the Dirac delta function, while for the Ritz-Galerkin method $w_k(x) = 1$ and $\varphi_k(x) = T_k(x)$. Note that the inner product of two real functions $g_1(t)$ and $g_2(t)$ is given by:

$$\langle g_1, g_2\rangle_{w_k} \equiv \int_{t=-1}^{1} w_k(t) g_1(t) g_2(t) dt \tag{18}$$

where $w_k(t)$ is a non-negative, real, integrable weight function.

Collocation method

Imposing the orthogonality concept displayed in (17), where $w_k(x) = \delta(x - x_k)$ and $\varphi_k(x) = 1$, on (16a) and (16b) produces:

$$\sum_{i=0}^{N} b_i^N T_i(x_k) = F_0^*(x_k) + \frac{\alpha\omega}{2}\left[a_0 \sum_{i=0}^{N} b_i^N I_{1,i}(x_k) + a_1 \sum_{i=0}^{N} c_i^N I_{2,i}(x_k)\right], \qquad k = 0, 1, \ldots, N \tag{19a}$$

and

$$\sum_{i=0}^{N} c_i^N T_i(x_k) = F_1^*(x_k) + \frac{\alpha\omega}{2}\left[a_0 \sum_{i=0}^{N} b_i^N I_{2,i}(x_k) + a_1 \sum_{i=0}^{N} c_i^N I_{3,i}(x_k)\right], \qquad k = 0, 1, \ldots, N \tag{19b}$$

where the integral functions $I_{n,i}(x)$, $n = 1, 2, 3$, $i = 0, 1, 2, \ldots, N$, are defined by:

$$I_{1,i}(x) \equiv \int_{x_0=-1}^{1} E_1(\alpha|x - x_0|) T_i(x_0) dx_0 \tag{20a}$$

$$I_{2,i}(x) \equiv \int_{x_0=-1}^{1} E_2(\alpha(x - x_0)) T_i(x_0) dx_0 - \int_{x_0=x}^{1} E_2(\alpha(x_0 - x)) T_i(x_0) dx_0 \tag{20b}$$

$$I_{3,i}(x) \equiv \int_{x_0=-1}^{1} E_3(\alpha|x - x_0|) T_i(x_0) dx_0 \tag{20c}$$

Here, x_j represents the collocation points in the finite set $\{x_k\}_{k=1}^{N}$. Through a lengthy but straightforward set of manipulations, one can show:

$$I_{n,i}(x) = 2(-1)^{r_n} \sum_{j=0}^{[i/2-r_n]} \left(\frac{1}{\alpha}\right)^{2j+r_n+1} \frac{1}{2j + r_n + n} T_i^{(2j+r_n)}(x)$$
$$- \sum_{j=0}^{i} \left(\frac{1}{\alpha}\right)^{j+1} T_i^{(j)}(1)[(-1)^i E_{j+n+1}(\alpha(1 + x)) + (-1)^{r_n} E_{j+n+1}(\alpha(1 - x))] \tag{21a}$$

where we have defined

$$r_n \equiv \begin{cases} 1, & n \text{ even} \\ 0, & n \text{ odd} \end{cases} \tag{21b}$$

Ritz-Galerkin method

We now proceed with the determination of the expansion coefficients of the Legendre moments of intensity using a Ritz-Galerkin method. As indicated previously, for the Ritz-Galerkin method we use $w_k(x) = 1$ and $\varphi_k(x) = T_k(x)$ in the restriction provided by (17). This provides a uniform weighting of the residual function over the entire interval as opposed to the discrete weighting associated with the collocation method.

From our analysis in the previous section, we can rewrite (16a), (16b) as:

$$R_0^N(x)+\sum_{i=0}^{N} b_i^N T_i(x)=F_0^*(x)+\frac{\alpha\omega}{2}\left[a_0\sum_{i=0}^{N} b_i^N I_{1,i}(x)+a_1\sum_{i=0}^{N} c_i^N I_{2,i}(x)\right] \tag{22a}$$

and

$$R_1^N(x)+\sum_{i=0}^{N} c_i^N T_i(x)=F_1^*(x)+\frac{\alpha\omega}{2}\left[a_0\sum_{i=0}^{N} b_i^N I_{2,i}(x)+a_1\sum_{i=0}^{N} c_i^N I_{3,i}(x)\right] \tag{22b}$$

where $I_{n,i}(x)$, $n=1,2,3$, $i=0,1,\ldots,N$, are given by (20a), (20b). After introducing our chosen functions for $w_k(x)$ and $\varphi_k(x)$ into the orthogonality condition shown in (17), we find:

$$\sum_{i=0}^{N} b_i^N A_{i,j}=\int_{x=-1}^{1} F_0^*(x)T_j(x)dx+\frac{\alpha\omega}{2}\left[a_0\sum_{i=0}^{N} b_i^N B_{1,i,j}+a_1\sum_{i=0}^{N} c_i^N B_{2,i,j}\right] \tag{23a}$$

$$\sum_{i=0}^{N} c_i^N A_{i,j}=\int_{x=-1}^{1} F_1^*(x)T_j(x)dx+\frac{\alpha\omega}{2}\left[a_0\sum_{i=0}^{N} b_i^N B_{2,i,j}+a_1\sum_{i=0}^{N} c_i^N B_{3,i,j}\right],\qquad j=0,1,\ldots,N \tag{23b}$$

where

$$A_{i,j}\equiv\int_{x=-1}^{1} T_i(x)T_j(x)dx,\qquad i,j=0,1,2,\ldots,N \tag{24}$$

which, with the aid of (11), can be expressed as[5,26]:

$$A_{i,j}=\begin{cases}\dfrac{1}{1-(i+j)^2}+\dfrac{1}{1-(i-j)^2}, & i+j\,\text{even}\\[2mm] 0, & i+j\,\text{odd}\end{cases} \tag{25}$$

and where

$$B_{n,i,j}\equiv\int_{x=-1}^{1} I_{n,i}(x)T_j(x)dx,\qquad i,j=0,1,\ldots,N,\ n=1,2,3 \tag{26}$$

After a straightforward set of manipulations, we arrive at:

$$\begin{aligned}B_{n,i,j}=\;&2(-1)^{r_n}\sum_{k=0}^{[i/2-r_n]}\left(\frac{1}{\alpha}\right)^{2k+r_n+1}\frac{1}{2k+r_n+n}\sum_{m=0}^{i-2k-r_n} d_{m,i,2k+r_n}A_{m,j}\\ &-[(-1)^{i+j}+(-1)^{r_n}]\sum_{k=0}^{i}\left(\frac{1}{\alpha}\right)^{k+1}T_i^{(k)}(1)J_{k+n+1,j}(1)\end{aligned} \tag{27a}$$

where

$$J_{n,j}(1)=\int_{x=-1}^{1} E_n(\alpha(1-x))T_j(x)dx \tag{27b}$$

and where we expressed $T_i^{(j)}(x)$ as a finite Chebyshev series, namely:

$$T_i^{(j)}(x)=\sum_{m=0}^{i-j} d_{m,i,j}T_m(x) \tag{28}$$

We note that $T_i^{(j)}(x)$ is simply a polynomial of order $(i-j)$. With the use of symbolic computation, the calculation of these coefficients is trivial and represents a one-time computation.

In the next section, error analysis is performed to quantify the accuracy of the proposed solutions.

ERROR ANALYSIS

After determining the expansion coefficients by the chosen method, the residuals are given by (16a), (16b). The size of the residuals provides us with an indication of the accuracy of the approximation, but we wish to calculate the errors in the functions $G_0^N(x)$ and $G_1^N(x)$ themselves.

Using our operator notation, (15a), (15b) are expressible as:

$$R_0^N = F_0^* + a_0\kappa_0 G_0^N + a_1\kappa_1 G_1^N - G_0^N \tag{29a}$$

and

$$R_1^N = F_1^* + a_0\kappa_1 G_0^N + a_1\kappa_2 G_1^N - G_1^N \tag{29b}$$

respectively. The exact solution produces no residual, that is,

$$0 = F_0^* + a_0\kappa_0 G_0^* + a_1\kappa_1 G_1^* - G_0^* \tag{30a}$$

$$0 = F_1^* + a_0\kappa_1 G_0^* + a_1\kappa_2 G_1^* - G_1^* \tag{30b}$$

Let us define the error as[5,27]:

$$\varepsilon_0^N \equiv G_0^* - G_0^N \tag{31a}$$

$$\varepsilon_1^N \equiv G_1^* - G_1^N \tag{31b}$$

By subtracting the corresponding equations in (29a), (29b) from those in (30a), (30b), and using the definitions of the errors, we obtain a relationship between the errors and the residuals, namely:

$$\varepsilon_0^N = R_0^N + a_0\kappa_0\varepsilon_0^N + a_1\kappa_1\varepsilon_1^N \tag{32a}$$

$$\varepsilon_1^N = R_1^N + a_0\kappa_1\varepsilon_0^N + a_1\kappa_2\varepsilon_1^N \tag{32b}$$

Unfortunately ε_0^N and ε_1^N are as inaccessible as the exact solutions G_0 and G_1, but the sizes of the errors may be measured by means of some functional norm.

We now introduce the concept of the functional norm, in particular the L_∞ norm. We may define this norm as:

$$\|\theta\|_\infty \equiv \operatorname*{Sup}_{x\in[-1,-]} |\theta(x)| \tag{33a}$$

for an arbitrary function $\theta(x)$. The infinity norm corresponds to the maximum absolute value that a function takes on in its domain of existence. The L_∞ norm of the errors expressed in (31a), (32b), therefore, is given as:

$$\|\varepsilon_j^N\|_\infty \operatorname*{Sup}_{x\in[-1,1]} |G_j^*(x) - G_j^N(x)|, \qquad j = 0, 1 \tag{33b}$$

This definition of the error is graphically depicted in *Figure 1*, where the maximum absolute error corresponds to the definition displayed in (33b). The corresponding infinity norm of the integral operator is expressible as[5,26]:

$$\|\kappa\|_\infty \equiv \operatorname*{Sup}_{x\in[-1,1]} \int_{x_0=-1}^{1} |k(x, x_0)| dx_0 \tag{33c}$$

where $k(x, x_0)$ is the kernel corresponding to the integral operator κ. Since we will consider only the infinity norm, we shall drop the subscripted "∞" in order to simplify the notation.

We shall use the following elementary results of functional analysis[28]:

$$\|A + B\| \leqslant \|A\| + \|B\| \qquad \|AB\| \leqslant \|A\| \times \|B\|$$
$$|\,\|A\| - \|B\|\,| \leqslant \|A - B\| \qquad \|aA\| = |a|\,\|A\| \tag{34a–d}$$

where A and B are any arbitrary functions and/or operators and where "a" is a scalar constant.

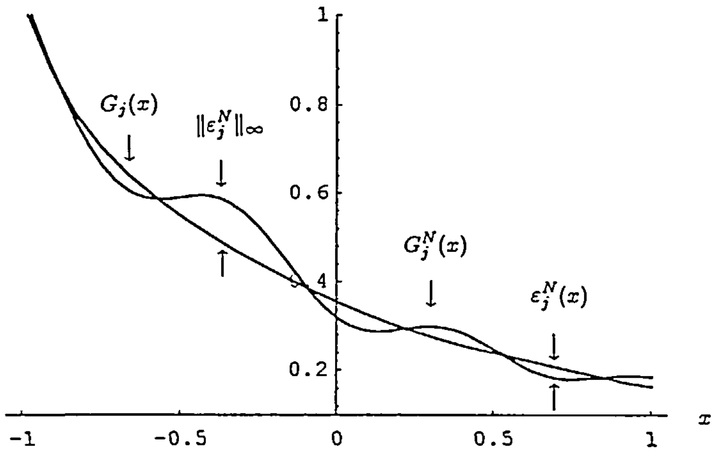

Figure 1 Schematic of the L_∞ norm of the error $\|\varepsilon_j^N\|_\infty$, between a function $G_j(x)$ and an approximation $G_j^N(x)$

Also, note from our definitions of the norm that $\|A\| \geqslant 0$. Then we begin our error bound calculations by considering (32a), (32b). Subtracting one from the other, we arrive at:

$$\varepsilon_0^N - \varepsilon_1^N = R_0^N - R_1^N + a_0(\kappa_0 - \kappa_1)\varepsilon_0^N + a_1(\kappa_1 - \kappa_2)\varepsilon_1^N \tag{35}$$

We now apply the definition of the infinity norm and, with the aid of (34a–d), we obtain:

$$\begin{aligned} |\|\varepsilon_0^N\| - \|\varepsilon_1^N\|| &\leqslant \|\varepsilon_0^N - \varepsilon_1^N\| \\ &\leqslant \|R_0^N - R_1^N\| + |a_0|\,\|\kappa_0 - \kappa_1\|\,\|\varepsilon_0^N\| + |a_1|\,\|\kappa_1 - \kappa_2\|\,\|\varepsilon_1^N\| \end{aligned} \tag{36}$$

The terms $\|\kappa_0 - \kappa_1\|$ and $\|\kappa_1 - \kappa_2\|$ represent the norms of the differences of the corresponding kernels. Note, however, that these are not equivalent to $\|\kappa_0\| - \|\kappa_1\|$ and $\|\kappa_1\| - \|\kappa_2\|$, respectively. In (36), we first consider the case that $\|\varepsilon_0^N\| \geqslant \|\varepsilon_1^N\|$. Then we may write:

$$0 \leqslant \|\varepsilon_0^N\| - \|\varepsilon_1^N\| \leqslant \|R_0^N - R_1^N\| + |a_0|\,\|\kappa_0 - \kappa_1\|\,\|\varepsilon_0^N\| + |a_1|\,\|\kappa_1 - \kappa_2\|\,\|\varepsilon_1^N\| \tag{37a}$$

or

$$\|\varepsilon_0^N\|[1 - |a_0|\,\|\kappa_0 - \kappa_1\|] + \|\varepsilon_1^N\|[-1 - |a_1|\,\|\kappa_1 - \kappa_2\|] \leqslant \|R_0^N - R_1^N\| \tag{37b}$$

This then yields the following inequality:

$$\|\varepsilon_1^N\| \geqslant \frac{r_1 - K_{01}\|\varepsilon_0^N\|}{-K_{11}} \tag{38a}$$

where we define

$$K_{01} \equiv [1 - |a_0|\,\|\kappa_0 - \kappa_1\|] \qquad K_{11} \equiv 1 + |a_1|\,\|\kappa_1 - \kappa_2\| \qquad r_1 = \|R_0^N - R_1^N\| \tag{38b–d}$$

Next, we consider the case that $\|\varepsilon_0^N\| < \|\varepsilon_1^N\|$. Then (36) gives us:

$$0 < \|\varepsilon_1^N\| - \|\varepsilon_0^N\| \leqslant \|R_0^N - R_1^N\| + |a_0|\,\|\kappa_0 - \kappa_1\|\,\|\varepsilon_0^N\| + |a_1|\,\|\kappa_1 - \kappa_2\|\,\|\varepsilon_1^N\| \tag{39a}$$

or

$$\|\varepsilon_0^N\|[-1 - |a_0|\,\|\kappa_0 - \kappa_1\|] + \|\varepsilon_1^N\|[1 - |a_1|\,\|\kappa_1 - \kappa_2\|] \leqslant \|R_0^N - R_1^N\| \tag{39b}$$

We thus attain:

$$\|\varepsilon_1^N\| \leqslant \frac{r_2 - K_{02}\|\varepsilon_0^N\|}{K_{12}} \tag{40a}$$

provided K_{12} is positive, where

$$K_{02} \equiv [-1 - |a_0|\,\|\kappa_0 - \kappa_1\|] \qquad K_{12} \equiv [1 - |a_1|\,\|\kappa_1 - \kappa_2\|]$$
$$r_2 \equiv \|R_0^N - R_1^N\| \tag{40b–d}$$

Next, we rearrange (30a), (30b) in the form:

$$R_0^N = \varepsilon_0^N - a_0\kappa_0\varepsilon_0^N - a_1\kappa_1\varepsilon_1^N \tag{41a}$$

$$R_1^N = \varepsilon_1^N - a_0\kappa_1\varepsilon_0^N - a_1\kappa_2\varepsilon_1^N \tag{41b}$$

Applying norms and using the relations given by (34a), (34d), we obtain:

$$\|R_0^N\| \leqslant \|\varepsilon_0^N\| + |a_0|\,\|\kappa_0\|\,\|\varepsilon_0^N\| + |a_1|\,\|\kappa_1\|\,\|\varepsilon_1^N\| \tag{42a}$$

$$\|R_1^N\| \leqslant \|\varepsilon_1^N\| + |a_0|\,\|\kappa_1\|\,\|\varepsilon_0^N\| + |a_1|\,\|\kappa_2\|\,\|\varepsilon_1^N\| \tag{42b}$$

Summing the two inequalities and simplifying, we arrive at:

$$\|R_0^N\| + \|R_1^N\| \leqslant \|\varepsilon_0^N\|[1 + |a_0|(\|\kappa_0\| + \|\kappa_1\|)] + \|\varepsilon_1^N\|[1 + |a_1|(\|\kappa_1\| + \|\kappa_2\|)] \tag{43}$$

We may therefore write:

$$\|\varepsilon_1^N\| \geqslant \frac{r_3 - K_{03}\|\varepsilon_0^N\|}{K_{13}} \tag{44a}$$

where

$$K_{03} \equiv [1 + |a_0|(\|\kappa_0\| + \|\kappa_1\|)] \qquad K_{13} \equiv [1 + |a_1|(\|\kappa_1\| + \|\kappa_2\|)]$$
$$r_3 \equiv \|R_0^N\| + \|R_1^N\| \tag{44b–d}$$

Once again we begin with (14a), (14b). Applying the norm to these equations we obtain:

$$\|\varepsilon_0^N\| \leqslant \|R_0^N\| + |a_0|\,\|\kappa_0\|\,\|\varepsilon_0^N\| + |a_1|\,\|\kappa_1\|\,\|\varepsilon_1^N\| \tag{45a}$$

and

$$\|\varepsilon_1^N\| \leqslant \|R_1^N\| + |a_0|\,\|\kappa_1\|\,\|\varepsilon_0^N\| + |a_1|\,\|\kappa_2\|\,\|\varepsilon_1^N\| \tag{45b}$$

Adding the two inequalities yields:

$$\|\varepsilon_0^N\| + \|\varepsilon_1^N\| \leqslant \|R_0^N\| + \|R_1^N\| + |a_0|(\|\kappa_0\| + \|\kappa_1\|)\|\varepsilon_0^N\| + |a_1|(\|\kappa_1\| + \|\kappa_2\|)\|\varepsilon_1^N\| \tag{46a}$$

which we may rewrite as:

$$\|\varepsilon_0^N\|[1 - |a_0|(\|\kappa_0\| + \|\kappa_1\|)] + \|\varepsilon_1^N\|[1 - |a_1|(\|\kappa_1\| + \|\kappa_2\|)] \leqslant \|R_0^N\| + \|R_1^N\| \tag{46b}$$

Thus we obtain:

$$\|\varepsilon_1^N\| \leqslant \frac{r_4 - K_{04}\|\varepsilon_0^N\|}{K_{14}} \tag{47a}$$

where

$$K_{04} \equiv [1 - |a_0|(\|\kappa_0\| + \|\kappa_1\|)] \qquad K_{14} \equiv [1 - |a_1|(\|\kappa_1\| + \|\kappa_2\|)]$$
$$r_4 \equiv \|R_0^N\| + \|R_1^N\| \tag{47b–d}$$

The relations given by (38a–d), (40a–d), (44a–d), and (47a–d) therefore provide us with a region in the first quadrant of the plane with abscissa $\|\varepsilon_0^N\|$ and ordinate $\|\varepsilon_1^N\|$ in which the errors must lie. This gives us a rigorous error bound for the cases in which the denominators of (40a) and (47a) are positive. An exemplary plot of this region will be provided in the results section.

RESULTS

Numerical results obtained using the Collocation and Ritz-Galerkin methods applied to the finite Chebyshev series approximations are compared to each other and to previously reported results obtained using other methods. Graphical representations of the Legendre moments of intensity and of the residual functions and errors are presented for the Chebyshev series solutions. Finally, convergence trends of the two methods are presented empirically for a specific example. All calculations and graphics presented here were performed with the symbolic computation software Mathematica™, version 2.0 for Windows™, and executed on a PC with 8 MBytes of memory.

We consider the case of uniform radiation of unit intensity incident on the boundary at $\tau = 0$ and no radiation incident at the boundary $\tau = \tau_D$. This gives us the boundary conditions $I(0, \mu) = 1$ and $I(\tau_D, -\mu) = 0$, $\mu > 0$, corresponding to (3a), (3b). We further assume that no internal sources are present, i.e., $s(\tau) = 0$. Therefore, the forcing functions of the integral form of the RTE reduce to $F_0(\tau) = E_2(\tau)$ and $F_1(\tau) = E_3(\tau)$, from (1c). We consider this case for comparison purposes since it is a classical problem and numerous results corresponding to this problem exist in the literature. For the collocation points, we use a closed, Gauss-Chebyshev rule[5,27], i.e. $x_k = \cos(\pi k/N)$, $k = 0, 1, \ldots, N$ which ensures that the residuals vanish at $x = \pm 1$.

The principle quantity of interest in engineering is the radiation heat flux, which can be expressed as $Q(x) = 2G_1(x)$. *Table 1* compares the radiation heat flux at the boundaries obtained

Table 1 Total radiation heat flux at the boundaries for different linearly anisotropic phase functions at different values of width $\tau_D = 1$

		ω					
		0.2		0.5		0.8	
a_1	Method	$Q(-1)$	$Q(1)$	$Q(-1)$	$Q(1)$	$Q(-1)$	$Q(1)$
0.643833	TC_6	0.96562	0.25344	0.89058	0.32758	0.76103	0.45553
	TG_6	0.96493	0.25356	0.89017	0.32752	0.76083	0.45538
	G_6	0.96564	0.25344	0.88981	0.32757	0.76075	0.45557
	TC_9	0.96564	0.25344	0.89060	0.32757	0.76105	0.45553
	F_9	0.96513	0.25397	0.88976	0.32843	0.76057	0.45588
	P_9	0.96780	0.25435	0.89151	0.32884	0.76192	0.45604
	DP_1	0.9648	0.2568	0.8889	0.3290	0.7587	0.4543
2.319461	TC_6	0.99221	0.27368	0.96735	0.39386	0.90592	0.59525
	TG_6	0.99152	0.27379	0.96695	0.39379	0.90569	0.59508
	G_6	0.99223	0.27368	0.96738	0.39386	0.90594	0.59525
	TC_9					0.90594	0.59525
	F_9					0.90406	0.60251
	P_9					0.90701	0.59596
2.602844	TC_6	0.99697	0.27734	0.98251	0.40719	0.93806	0.62650
	TG_6	0.99628	0.27746	0.98211	0.40712	0.93783	0.62632
	G_6	0.99698	0.27734	0.98254	0.40718	0.93808	0.62650
	TC_9					0.93808	0.62650
	F_9					0.94178	0.63874
	P_9					0.93920	0.62726
	DP_1					0.9336	0.6231

Table 2 Effect of optical thickness on the radiative flux Q at the boundaries for $a_1 = 2.602844$, $\omega = 0.8$

	τ_D					
	0.1		2.0		10.0	
Method	$Q(-1)$	$Q(1)$	$Q(-1)$	$Q(1)$	$Q(-1)$	$Q(1)$
TC_6	0.98085	0.94234	0.93048	0.41647	0.92177	0.01741
TG_6	0.98087	0.94235	0.92975	0.41593	0.91599	0.01328
G_6	0.98085	0.94234	0.92938	0.41672	0.91005	0.02230
F_1	0.99293	0.95838	0.93336	0.43903	0.92011	0.02216
F_9	0.98692	0.94856	0.92523	0.43029	0.91332	0.02454
P_9	0.98885	0.95020	0.92660	0.43072	0.91464	0.02456
DP_1	0.9777	0.9388	0.9285	0.4171	0.9228	0.0170

from the finite Chebyshev series approximation for both the collocation and Ritz-Galerkin methods to results obtained by other methods. A Galerkin method similar to that presented here was utilized by Krim[6], and is used as the standard for comparison in this study. Three different phase functions are considered and solutions for different values of the single-scattering albedo ω are given for an optical thickness of $\tau_D = 1$. The Chebyshev collocation method is indicated by TC while the Chebyshev Ritz-Galerkin is denoted by TG. The Galerkin approach presented by Krim[6] is denoted by G. Results from the F_N[6] and P_N[14] methods are also included, as are those of the double-spherical harmonics (DP) method[7]. The F_N and P_N methods, in the past, have served as benchmarks for comparison and as such, are included for cases where results were available. The numerical subscripts represent the order of the approximation used in each case. The F_N method has generally been considered to produce the most accurate results of any other method.

It is interesting to note that the collocation method results tend to agree more closely to the weighted Galerkin results G_6 than the higher order Chebyshev Ritz-Galerkin results. This fact makes the TC method quite favourable over the other two due to the computational simplicity of this approach. The TC results seem also to confirm the accuracy of these figures. In light of the similarity between these three approximations, however, the accuracy of the F_9 and P_9 appear to be in error.*

We see in this table that as the single-scattering albedo ω is increased, the radiative flux decreases at the left boundary while it increases at the right boundary, due to the increased role of the (forward) scattering. The radiant energy is thus scattered forward rather than being absorbed within the medium. Similarly, as a_1 increases, the scattering becomes more highly forward and the back scattering is reduced. This results in less of the incident radiation being scattered back out and more energy passing into and through the medium. Therefore, the radiative flux is increased at both boundaries as compared to the flux for a smaller value of a_1 with fixed ω.

In *Table 2*, we illustrate the effect of the optical thickness on the radiation heat flux and compare the results to different methods. The results presented correspond to a value of $a_1 = 2.602844$ with $\omega = 0.8$. From the table, we see that as the optical thickness is increased, the radiative flux decreases at the boundaries, due to absorption and scattering within the medium.

Table 3 compares the zeroth Legendre moment of intensity obtained from the Chebyshev collocation and Ritz-Galerkin methods to results reported by Krim[6]. Again, it is seen that the Chebyshev collocation method gives results which are in excellent agreement with the higher order method G_6 over a large range of values for a_1, τ_D, and ω.

* This was apparently shown by Siewart. This was related to authors by a reviewer.

Table 3 Zeroth Legendre moment of intensity at right boundary, $G_0^N(1)$, at different optical depths for $a_1 = 0.643833$ and $a_1 = 2.602844$ and different values of ω

a_1	ω	Method	τ_D 0.1	1.0	2.0
0.643833	0.2	TC_6	0.74841	0.18021	0.05103
		TG_6	0.75484	0.18318	0.05639
		G_6	0.74841	0.18019	0.05098
	0.5	TC_6	0.79045	0.25117	0.08885
		TG_6	0.78898	0.25444	0.09360
		G_6	0.79046	0.25116	0.08878
	0.8	TC_6	0.83696	0.37749	0.18748
		TG_6	0.83796	0.38179	0.19273
		G_6	0.83696	0.37752	0.18751
2.602844	0.2	TC_6	0.75602	0.19889	0.06146
		TG_6	0.76016	0.20188	0.06678
		G_6	0.75602	0.19888	0.06141
	0.5	TC_6	0.81013	0.31619	0.13775
		TG_6	0.80822	0.31978	0.14294
		G_6	0.81013	0.31618	0.13769
	0.8	TC_6	0.86948	0.52311	0.34235
		TG_6	0.87052	0.52869	0.35022
		G_6	0.76948	0.52316	0.34246

We present in *Figure 2* plots of the zeroth Legendre moment of intensity along with the resulting residuals and errors for the case where $\tau_D = 1.0$, $\omega = 0.8$, $N = 6$, and $a_1 = 0.643833$ obtained by the collocation method, and in *Figure 3* we present a similar plot for the Ritz-Galerkin method. The error was calculated numerically using a product integration[27] trapezoid rule with 161 equally spaced points. *Figures 4* and *5* include plots for the first Legendre moment of intensity and the resulting residuals and errors for the case where $\tau_D = 1.0$, $\omega = 0.8$, $N = 6$, and $a_1 = 0.643833$ for the collocation and Ritz-Galerkin methods, respectively.

The region obtained from the error bounds represented by (38a–d), (40a–d), (44a–d) and (47a–d) is plotted for the collocation method in *Figure 6* and for the Ritz-Galerkin method in *Figure 7*, both for the case corresponding to $N = 6$, $\tau_D = 1.0$, $\omega = 0.8$, and $a_1 = 0.643833$. For the collocation method, the location of the numerically calculated error norms can be seen to lie roughly in the centre of the corresponding region, as indicated in *Figure 6*, while for the Ritz-Galerkin method, the location of these norms is in the low centre portion of *Figure 7*. From *Figures 3(b)* through *6(b)* it is clear that the L_∞ norm of the residuals is greater for the Ritz-Galerkin method than for the collocation method. As a result, the L_∞ norm of the errors is expected to be correspondingly greater for the Ritz-Galerkin method. This is indeed the case for $\|\varepsilon_0^N\|$, based on the numerical calculation of the errors. However, $\|\varepsilon_1^N\|$ is actually smaller in the case of the Ritz-Galerkin solution. This is clearly due to the smaller residual over the interior portion of the domain in the Ritz-Galerkin method. An analysis of the errors using some other norm, for example the L_2 norm, may more accurately illustrate this effect.

Figures 8 and *9* show the region of the error bound for the collocation and Ritz-Galerkin methods, respectively, for three different values of N in order to show the rates of convergence for the two methods. It is interesting that the polygons which represent the error bounds appear geometrically similar for different values of N, although based on the actual bound inequalities, it was found that the polygons are not truly similar. The convergence rates for the two methods are essentially identical, based on the figures, although the collocation method does have slightly tighter bounds for this case.

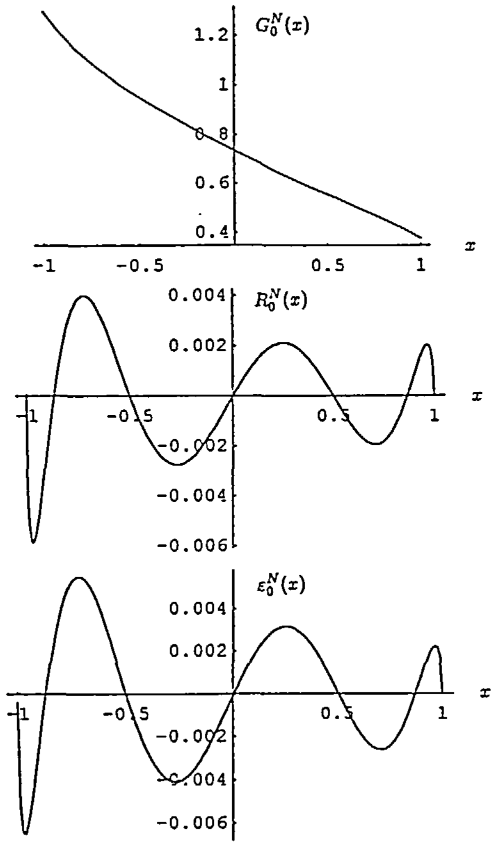

Figure 2 Plot of the zeroth Legendre moment of intensity obtained by the collocation method along with the resulting residuals and errors for the case where $N = 6$, $\tau_D = 1.0$, $\omega = 0.8$, and $a_1 = 0.643833$

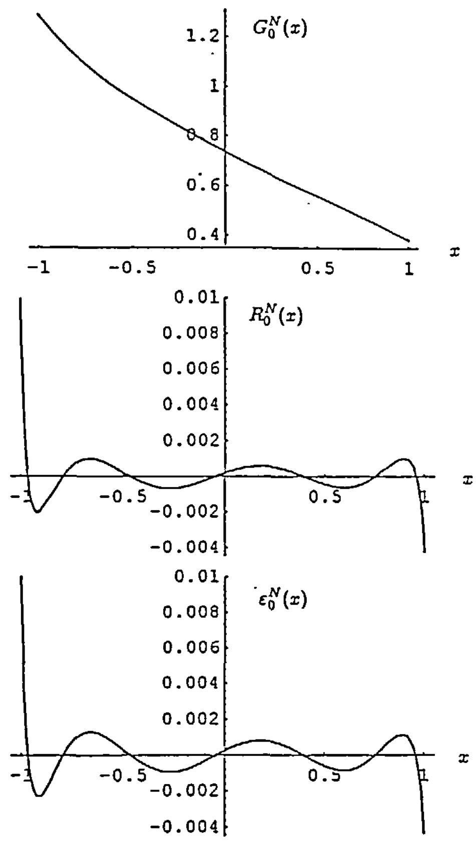

Figure 3 Plot of the zeroth Legendre moment of intensity obtained by the Ritz-Galerkin method along with the resulting residuals and errors for the case where $N = 6$, $\tau_D = 1.0$, $\omega = 0.8$, and $a_1 = 0.643833$

From the error plots in *Figures 2* through *5*, we see that the average error resulting from the Ritz-Galerkin method may be smaller than that arising from the collocation method. The maximum residual occurs at the boundary for the Ritz-Galerkin method, and as a result the maximum error may be expected to occur there as well. In much of the literature, accuracy of results has been measured by comparing the Legendre moments of intensity (or radiative fluxes) which occur at the boundaries. Since the largest errors may occur at the boundaries, this may be a rather poor measurement. The collocation method, on the other hand, produces zero residual at the boundaries if the boundary points are used as collocation points, and as a result the error there is quite small. Therefore, without performing a detailed error analysis, the accuracy of any given method may be improperly interpreted if boundary results are the only means of comparison.

The suitability of one method over another may depend on the purpose of the radiation analysis. For example, if the solution to a radiation problem is required to obtain the boundary condition for a conduction/convection problem, then accurate boundary radiation heat fluxes are required and the collocation method may produce the best results. On the other hand, if one desires the temperature distribution within a medium in which radiation is significant, then accurate boundary results alone will not suffice.

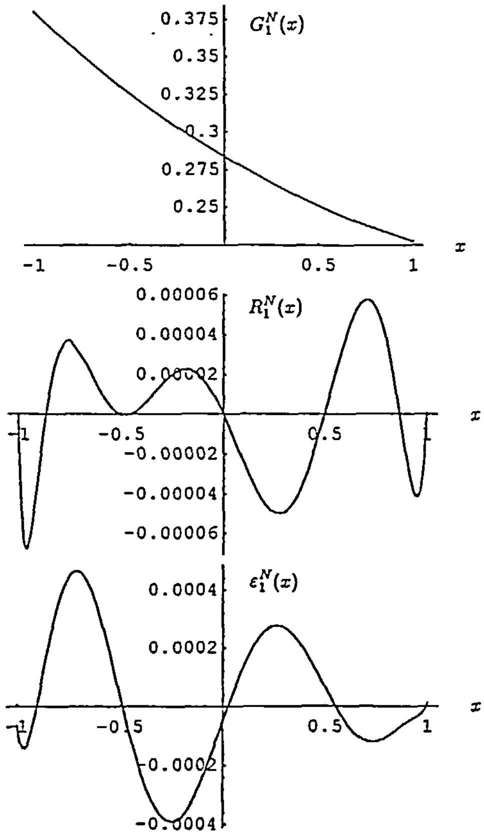

Figure 4 Plot of the first Legendre moment of intensity obtained by the collocation method along with the resulting residuals and errors for the case where $N = 6$, $\tau_D = 1.0$, $\omega = 0.8$, and $a_1 = 0.643833$

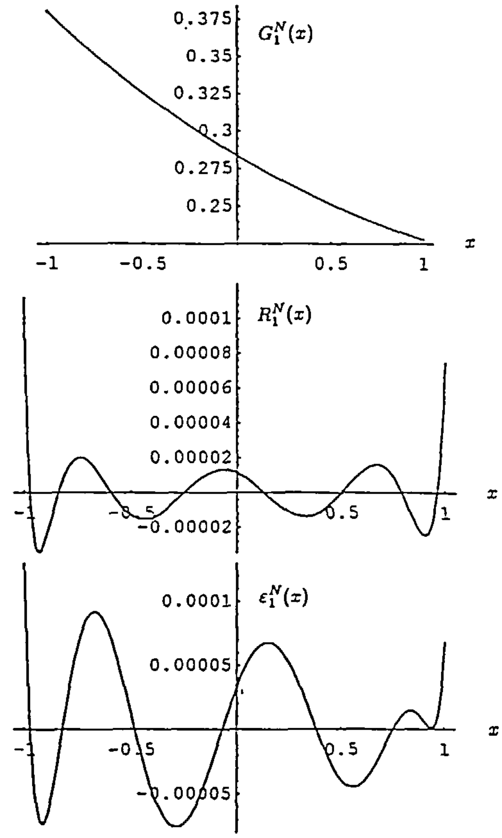

Figure 5 Plot of the first Legendre moment of intensity obtained by the Ritz-Galerkin method along with the resulting residuals and errors for the case where $N = 6$, $\tau_D = 1.0$, $\omega = 0.8$, and $a_1 = 0.643833$

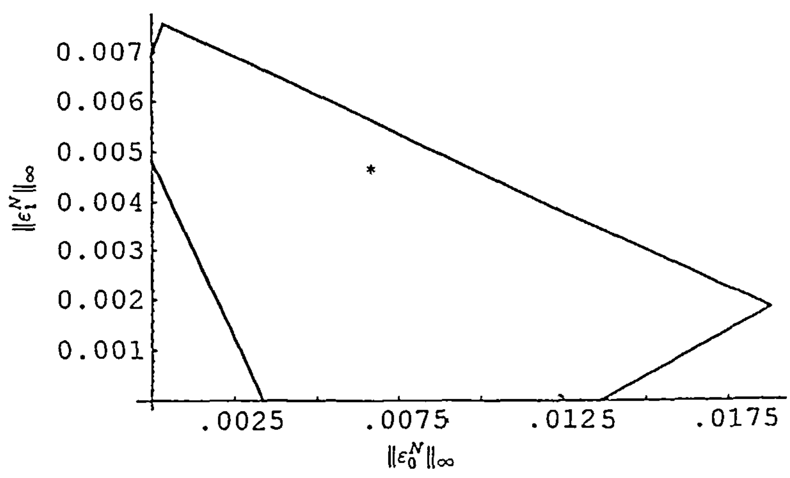

"*" denotes the location of the numerically calculated error norms.

Figure 6 Error bound for the collocation method for the case where $N = 6$, $\tau_D = 1.0$, $\omega = 0.8$, and $a_1 = 0.643833$

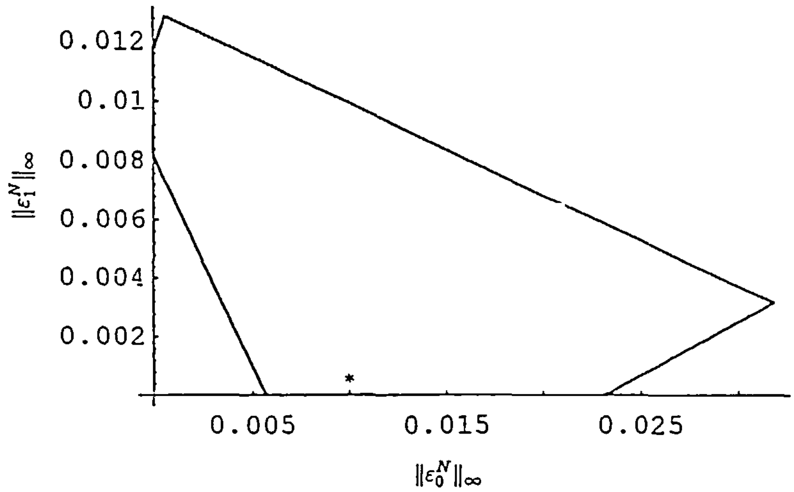

Figure 7 Error bound for the Ritz-Galerkin method for the case where $N = 6$, $\tau_D = 1.0$, $\omega = 0.8$, and $a_1 = 0.643833$

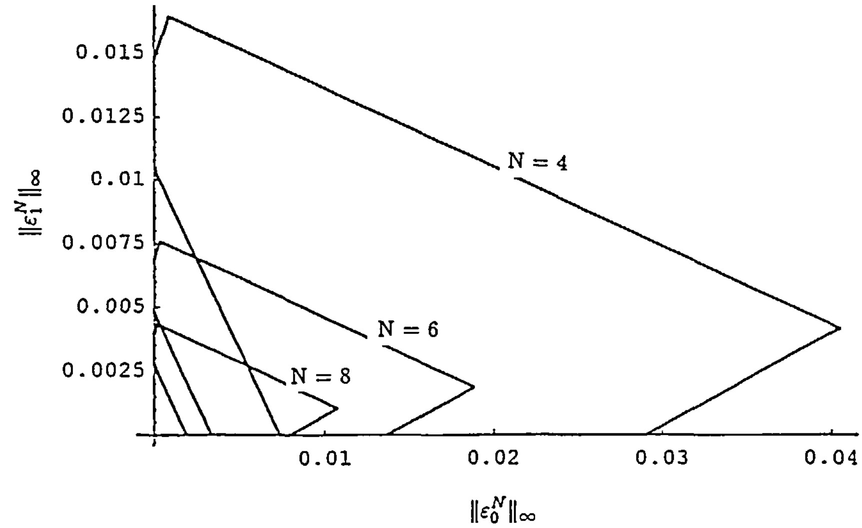

Figure 8 Comparison of the region of the error bound for increasing values of N for the collocation method for the case where $\tau_D = 1.0$, $\omega = 0.8$, and $a_1 = 0.643833$

In *Table 4*, we compare the expansion coefficients which are obtained using the collocation method for the case where $\tau_D = 1.0$, $\omega = 0.8$, and $a_1 = 0.643883$, for different values of N, in order to show convergence trends for this method. In *Table 5* the same comparison is made for the Ritz-Galerkin method. It is interesting to note that the leading coefficients—b_0^N and c_0^N—are within less than one percent of their corresponding values for $N = 4$ and $N = 10$ in the Ritz-Galerkin Method, while the convergence is much slower for the collocation method.

From these results, it is apparent that the collocation method provides excellent results at the boundaries of the domain. However, within the interior the Ritz-Galerkin method may provide

Table 4 Comparison of expansion coefficients obtained from the collocation method for the case where $\tau_D = 1.0$, $\omega = 0.8$, and $a_1 = 0.643833$ for several values of N

	$N = 4$		$N = 6$		$N = 8$		$N = 10$	
i	b_i^N	c_i^N	b_i^N	c_i^N	b_i^N	c_i^N	b_i^N	c_i^N
0	0.23466	0.22866	0.75549	0.29125	0.78028	0.29372	0.78024	0.29372
1	0.33174	−0.04199	−0.38730	−0.07330	−0.42913	−0.07563	−0.42894	−0.07562
2	−0.38668	−0.00305	0.01328	0.00849	0.04813	0.01020	0.04802	0.01020
3	0.17056	0.00378	0.00649	0.00057	−0.02147	−0.00072	−0.02124	−0.00072
4	−0.04492	−0.00070	−0.01509	−0.00065	0.00524	0.00022	0.00509	0.00034
5			0.00762	0.00043	−0.00534	−0.00004	−0.00499	−0.00004
6			−0.00492	−0.00013	0.00189	0.00004	0.00165	0.00003
7					−0.00276	9.5×10^{-6}	−0.00213	-9.2×10^{-6}
8					0.00067	−0.00004	0.00086	0.00001
9							−0.00138	5.7×10^{-6}
10							0.00034	−0.00002

Table 5 Comparison of expansion coefficients obtained from the Ritz-Galerkin method for the case where $\tau_D = 1.0$, $\omega = 0.8$, and $a_1 = 0.643833$ for several values of N

	$N = 4$		$N = 6$		$N = 8$		$N = 10$	
i	b_i^N	c_i^N	b_i^N	c_i^N	b_i^N	c_i^N	b_i^N	c_i^N
0	0.77980	0.29368	0.78003	0.29371	0.78003	0.29391	0.78002	0.29333
1	−0.42621	−0.07560	−0.42785	−0.07562	−0.42896	−0.07562	−0.42834	−0.07005
2	0.04712	0.01010	0.04760	0.01018	0.04760	0.01059	0.04758	0.00940
3	−0.01816	−0.00070	−0.02007	−0.00071	−0.02127	−0.00072	−0.02060	0.00512
4	0.00406	0.00006	0.00463	0.00018	0.00463	0.00063	0.00460	−0.00067
5			−0.00363	−0.00003	−0.00509	−0.00003	−0.00427	0.00647
6			0.00109	−0.00001	0.00109	0.00055	0.00105	−0.00107
7					−0.00281	-6.1×10^{-6}	−0.00122	0.00812
8					4.4×10^{-6}	0.00102	−0.00014	−0.00203
9							−0.00003	0.01536
10							0.00025	-2.2×10^{-8}

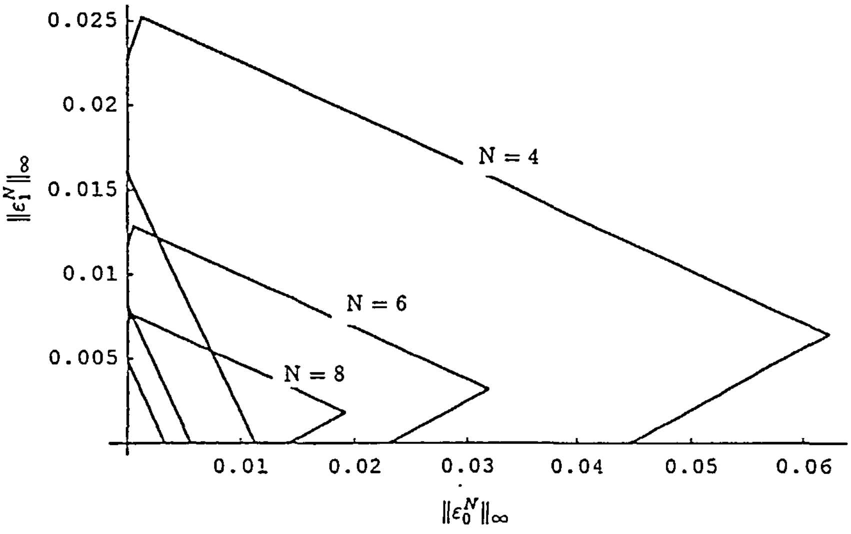

Figure 9 Comparison of the region of the error bound for increasing values of N for the Ritz-Galerkin method for the case where $\tau_D = 1.0$, $\omega = 0.8$, and $a_1 = 0.643833$

somewhat more reliable results. Both methods provide results which are within one percent of the values obtained by other methods and therefore should be acceptable for most engineering applications. Since the collocation method requires much less computational effort, this may be preferable over the other methods.

CONCLUSIONS

The problem of one-dimensional radiation in a medium which absorbs, emits, and scatters radiation subjected to uniform incident radiation at one of the boundaries and with no internal emission source was solved for the case of a linearly anisotropic scattering phase function using the integral form of the transport equation. After transforming the domain via a linear transformation, the unknown functions were approximated by a finite Chebyshev series solution. Two separate orthogonality conditions were applied to the residual functions resulting from the approximation to obtain the two separate methods, collocation and Ritz-Galerkin, for determining the unknown expansion coefficients.

Following determination of the expansion coefficients, the residuals were calculated and error bounds were obtained from these residuals. This provided us with a quantitative means of analyzing the accuracy of the approximation. The results obtained were also compared to those obtained using other methods, and the benefits of the different methods were discussed as well as applications for which one method might be more suitable than another. It was found that the collocation method produced quite accurate results by using closed rule Chebyshev-Lobatto collocation points. Due to the relative ease in numerical computation, this method appears to be quite applicable to a variety of applications.

ACKNOWLEDGEMENTS

Partial funding for this work was provided by a NASA Space Research Assistantship Program to T. LaClair and by the Department of Energy (DE-FG05-93ER25173)

REFERENCES

1 Viskanta, R. Radiation heat transfer: interaction with conduction and convection and approximate methods in radiation, *Heat Transfer—Proc. of the 7th Int. Heat Transfer Conf.*, **2**, 103–121 (1982)
2 Chandrasekhar, S. *Radiative Transfer*, Dover, New York (1960)
3 Mengüc, M. P. and Viskanta, R. Comparison of radiative transfer approximations for highly forward scattering planar medium, *J. Quant. Spectr. Rad. Trans.*, **29**, 381–394 (1983)
4 Thynell, S. T. and Özisik, M. N. Use of eigenfunctions for solving radiation transfer in anisotropically scattering, plane-parallel media, *J. Appl. Phys.*, **60**, 541–551 (1986)
5 Frankel, J. I. Several symbolic augmented Chebyshev expansions for solving the equation of radiative transfer, *J. Comp. Physics* (in press)
6 Abdel Krim, M. S. Radiation transfer for linearly anisotropic phase functions, *Astrophys. Space Sci.*, **164**, 69–77 (1990)
7 Kumar, S. and Felske, J. D. Radiative transport in a planar medium exposed to azimuthally unsymmetric incident radiation, *J. Quant. Spectr. Rad. Trans.*, **35**, 187–212 (1986)
8 Frankel, J. I. Computational attributes of the integral form of the equation of transfer, *J. Quant. Spectr. Rad. Trans.*, **46**, 329–342 (1991)
9 Case, K. M. and Zweifel, P. F. *Linear Transport Theory*, Addison-Wesley, Reading, MA (1967)
10 Ozisik, M. N. *Radiative Transfer*, Wiley, New York (1980)
11 Duderstadt, J. J. and Martin, W. R. *Transport Theory*, Wiley, New York (1979)
12 McCormick, N. J. and Mendelson, M. R. Transport solution of the one-speed slab albedo problem, *Nucl. Sci. Engng.*, **20**, 462–467 (1964)
13 Siewert, C. E. The F_N method for solving radiative-transfer problems in plane geometry, *Astro. Apace Sci.*, **58**, 131–137 (1978)
14 Benassi, M., Cotta, R. M. and Siewert, C. E. The P_N method for radiative transfer problems with reflective boundary conditions, *JQSRT*, **30**, 547–553 (1983)
15 Ozisik, M. N. and Yener, Y. The Galerkin method for solving radiation transfer in plane-parallel participating media, *J. Heat Transfer*, **104**, 351–354 (1982)
16 Cengel, Y. A., Ozisik, M. N. and Yener, Y. Determination of angular distribution of radiation in an isotropically scattering slab, *J. Heat Transfer*, **106**, 248–252 (1984)
17 Cengel, Y. A. and Ozisik, M. N. Radiation transfer in an anisotropically scattering slab with directional dependent reflectivities, *ASME Paper 86-HT-28* (1986)
18 Sutton, W. H. and Ozisik, M. N. A Fourier transform solution for radiative transfer in a slab with isotropic scattering and boundary reflection, *JQSRT*, **22**, 55–64 (1979)
19 Thynell, S. T. and Ozisik, M. N. Use of eigenfunctions for solving radiation transfer in anisotropically scattering, plane-parallel media, *J. Appl. Phys.*, **60**, 541–551 (1986)
20 Abramowitz, M. and Stegun, I. A. *Handbook of Mathematical Functions*, Dover, New York (1965)
21 Rivlin, T. J. *The Chebyshev Polynomials*, Wiley, New York (1974)
22 Frankel, J. I. A Galerkin solution to a regularized Cauchy singular integro-differential equation, *Quart. Appl. Math.*, (in press).
23 Porter, D. and Stirling, D. S. G. *Integral Equations*, Cambridge University Press, Cambridge (1990)
24 Golberg, M. A., ed. *Solution Methods for Integral Equations*, Plenum Press, New York (1979)
25 Golberg, M. A., ed. *Numerical Solution of Integral Equations*, Plenum Press, New York (1990)
26 Delves, L. M. and Mohamed, J. L. *Computational Methods for Integral Equations*, Cambridge Univ. Press, Cambridge (1988)
27 Atkinson, K. E. *A Survey of Numerical Methods for the Solution of Fredholm Integral Equations of the Second Kind*, Society for Industrial and Applied Mathematics, Philadelphia (1976)
28 Riesz, F. and Sz.-Nagy, B. *Functional Analysis*, Frederick Ungar Publishing, New York (1955)